Title

Phospho-valproic acid (MDC-1112) suppresses glioblastoma growth in preclinical models through the inhibition of STAT3 phosphorylation

Journal

Carcinogenesis, 40(12)

ISSN

0143-3334

Authors

Luo, Dingyuan
Fraga-Lauhirat, Magdalena
Millings, Jonathan
et al.

Publication Date

2019-12-31

DOI

10.1093/carcin/bgz069

Peer reviewed

Carcinogenesis, 2019, 1–12

doi:10.1093/carcin/bgz069
Advance Access publication April 17, 2019
Original Article

ORIGINAL ARTICLE

Phospho-valproic acid (MDC-1112) suppresses glioblastoma growth in preclinical models through the inhibition of STAT3 phosphorylation

Dingyuan Luo[1–3,†], Magdalena Fraga-Lauhirat[1,†], Jonathan Millings[4], Cristella Ho[1], Emily M.Villarreal[1], Teresa C.Fletchinger[1], James V.Bonfiglio[4], Leyda Mata[4], Matthew D.Nemesure[4], Lauren E.Bartels[4], Ruixue Wang[4], Basil Rigas[5,6] and Gerardo G. Mackenzie[1,4,*]

[1]Department of Nutrition, University of California, One Shields Ave, Davis, CA 95616, USA, [2]Department of Thyroid Surgery and [3]Guangdong Provincial Key Laboratory of Malignant Tumor Epigenetics and Gene Regulation, Medical Research Center, Sun Yat-Sen Memorial Hospital, Sun Yat-Sen University, Guangzhou 510120, China and [4]Department of Family, Population and Preventive Medicine, [5]Department of Medicine and [6]Stony Brook Cancer Center, Stony Brook University, Stony Brook, NY 11794-8175, USA

*To whom correspondence should be addressed. Tel: +530 752 2140; Fax: +530 752 8966; Email: ggmackenzie@ucdavis.edu
†These authors contributed equally to this work.

Abstract

New therapeutic strategies against glioblastoma multiforme (GBM) are urgently needed. Signal transducer and activator of transcription 3 (STAT3), constitutively active in many GBM tumors, plays a major role in GBM tumor growth and represents a potential therapeutic target. We have documented previously that phospho-valproic acid (MDC-1112), which inhibits STAT3 activation, possesses strong anticancer properties in multiple cancer types. In this study, we explored the anticancer efficacy of MDC-1112 in preclinical models of GBM, and evaluated its mode of action. MDC-1112 inhibited the growth of multiple human GBM cell lines in a concentration- and time-dependent manner. Normal human astrocytes were resistant to MDC-1112, indicating selectivity. *In vivo*, MDC-1112 reduced the growth of subcutaneous GBM xenografts in mice by up to 78.2% ($P < 0.01$), compared with the controls. Moreover, MDC-1112 extended survival in an intracranial xenograft model. Although all vehicle-treated mice died by 19 days of treatment, 7 of 11 MDC-1112-treated mice were alive and healthy by the end of 5 weeks, with many showing tumor regression. Mechanistically, MDC-1112 inhibited STAT3 phosphorylation at the serine 727 residue, but not at tyrosine 705, *in vitro* and *in vivo*. STAT3 overexpression rescued GBM cells from the cell growth inhibition by MDC-1112. In addition, MDC-1112 reduced STAT3 levels in the mitochondria and enhanced mitochondrial levels of reactive oxygen species, which triggered apoptosis. In conclusion, MDC-1112 displays strong efficacy in preclinical models of GBM, with the serine 727 residue of STAT3 being its key molecular target. MDC-1112 merits further evaluation as a drug candidate for GBM.

Introduction

Glioblastoma multiforme (GBM), the most common primary malignant brain tumor, is a devastating disease (1). Despite an aggressive standard-of-care regimen combining maximum safe surgical resection plus radiation therapy and chemotherapy (temozolomide), the median progression-free survival is ~7 months, the median overall survival is 15 months, and the 2-year overall survival is 27% (2,3). Despite extensive efforts to improve GBM therapy, the prognosis of the patients continues

Received: December 14, 2018; **Revised:** March 22, 2019; **Accepted:** April 15, 2019

Abbreviations

GBM	glioblastoma multiforme
NHA	normal human astrocytes
PBS	phosphate-buffered saline
ROS	reactive oxygen species
Ser727	serine 727
STAT3	signal transducer and activator of transcription 3
Tyr705	tyrosine 705
VPA	valproic acid

to be dismal (3,4). Thus, there is an urgent need to develop new agents against GBM.

The signal transducer and activator of transcription 3 (STAT3) transcription factor is a major intracellular signaling protein, regulating important biological functions, such as cell proliferation, differentiation, survival, angiogenesis and immune response (5). STAT3 signaling activation involves the formation of a signaling-competent receptor complex that upon binding activates the receptor-associated Janus family of tyrosine kinases (6). Janus family of tyrosine kinases phosphorylate STAT proteins that once phosphorylated at the tyrosine 705 (Tyr705) residue form homo- or heterodimers. This allows its translocation to the nucleus, where it regulates the transcription of multiple proteins related to inflammation and cancer (7). Besides Tyr705 phosphorylation, STAT3 is also activated by serine 727 (Ser727) phosphorylation, where it mediates the actions of mitochondrial STAT3 in controlling respiration and Ras-dependent transformation (8,9).

Constitutive activation of STAT3 is important in oncogenic signaling and occurs at high frequency in human cancers, including GBM (5,10). Activation of STAT3 in GBM correlates with malignancy and poor prognosis, and has been shown to be essential to the maintenance of GBM stem cells (11). Furthermore, constitutive activation of STAT3 in gliomas is positively associated with tumor grade (12,13). In particular, high expression of phosphorylated STAT3, at both Tyr 705 and Ser727 residues, has been detected in human GBM specimens and both were predictive of poorer clinical outcome; however, only the high proportion of phosphorylated STAT3 Ser727 positive neoplastic cells in GBM was shown to be an independent unfavorable prognostic factor (14). Moreover, inhibition of STAT3 enhances the radiosensitizing effect of temozolomide in GBM (15). These data clearly indicate that STAT3 represents a potential target for GBM treatment (16).

We have identified previously the new agent MDC-1112 (Figure 1A) as a potent STAT3 inhibitor (17). We have shown that MDC-1112 is effective in inhibiting the growth of pancreatic cancer in mice, through the inhibition of STAT3 at the cytosolic and mitochondrial level (17). This novel agent has been synthesized based on a general approach where a specific chemical modification of known drugs enhances their desired anticancer properties, primarily their efficacy (18,19).

In the current work we examined, for the first time, the efficacy of MDC-1112 in preclinical models of GBM and explored its mode of action. Our data show that MDC-1112 strongly inhibited the growth of subcutaneous GBM murine xenografts; extended survival of mice bearing intracranial tumors; reduced STAT3 phosphorylation selectively at the Ser727 residue, leading to a decrease in mitochondrial STAT3 levels; enhanced the generation of reactive oxygen species (ROS) by the mitochondria and induced GBM cell death by apoptosis.

Materials and methods

Reagents

MDC-1112 (Figure 1A) was a gift from Medicon Pharmaceuticals (Stony Brook, NY). MDC-1112 was prepared as a 100-mM stock solution in sterile dimethyl sulfoxide. Valproic acid (VPA) was purchased from Sigma–Aldrich (St Louis, MO). Annexin V-FITC was purchased from Invitrogen (Carlsbad, CA). All general solvents and reagents were of HPLC grade or the highest grade commercially available.

Cell culture and cell growth assay

Human GBM cell lines [U87, LN-18, LN-229, U118; American Type Culture Collection (ATCC), Manassas, VA] were grown as monolayers in the medium suggested by ATCC and supplemented with 10% fetal bovine serum (Mediatech, Herndon, VA), penicillin (50 U/ml) and streptomycin (50 μg/ml; Life Technologies, Grand Island, NY). Cells were grown in a humidified incubator at 37°C with 5% CO_2. We have not authenticated these cell lines, however we routinely test each cell line every 3 months for mycoplasma contamination. All the cell lines were characterized by cell morphology and growth rate and passaged in our laboratory <6 months after being received. Normal human astrocytes (NHA) were obtained from Lonza (Walkersville, MD) and cultured in astrocyte basal growth medium, supplemented with 25 μg/ml bovine insulin, 20 ng/ml epidermal growth factor, 5% fetal bovine serum, 20 ng/ml progesterone and 50 μg/ml transferrin.

To determine cell growth, NHA and GBM cells were treated with various concentrations of MDC-1112 for 24, 48 or 72 h. Following treatment, the reduction of 3-(4,5-dimethylthiazol-2-yl)-2,5-diphenyl tetrazolium bromide dye (MTT) was monitored, as described previously (20).

Clonogenic assay

This was performed as described previously (21). Briefly, U87 and LN-18 cells, plated in 6-well plates (1000 cells per well), were treated with MDC-1112 for 24 h. Following treatment, cells were grown for 10 days, with their media replaced every 3 days. Cells were then stained with 1% crystal violet in borate-buffered saline (0.1 M, pH 9.3) and 0.02% ethanol, and colonies were counted.

Apoptosis

GBM cells (1.0×10^5 cells per well) were treated with various concentrations of MDC-1112 for 24 h. Briefly, after treatment with the test agent, cells were trypsinized, stained with Annexin V-FITC (100X dilution; Invitrogen) and propidium iodide (0.5 μg/ml; Sigma), and the fluorescence intensities were analyzed by FACSCalibur (BD Bioscience).

Determination of mitochondrial superoxide by FACSCalibur

LN-18 and U87 cells (1.0×10^5 cells per well) were incubated in the presence of 1× or 2 × IC_{50} MDC-1112 or VPA or equivalent volumes of dimethyl sulfoxide for 1 h. After treatment with the test drug, cells were trypsinized and stained with 10-μM MitoSOX Red for 30 min at 37°C and the fluorescence intensity was analyzed by FACSCalibur (BD Bioscience).

Determination of mitochondrial superoxide by fluorescence microscopy

LN-18 and U87 cells were seeded overnight in glass bottom culture dishes (MatTek, Ashland, MA) and incubated in the presence of 1 × IC_{50} MDC-1112 or VPA or equivalent volumes of dimethyl sulfoxide for 0, 30, 60 or 120 min. Following treatment, mitochondrial superoxide was determined by fluorescence microscopy as described previously (22).

Determination of mitochondrial membrane potential

LN-18 and U87 cells were incubated with 1.5 × IC_{50} MDC-1112 for 3 h. The mitochondrial membrane potential was determined by flow cytometry using the JC-1 cationic dye (5,5′,6,6′-tetrachloro-1,1′,3,3′- tetraethylbenzimidazolylcarbocyanine iodide; Invitrogen), as described previously (23).

A

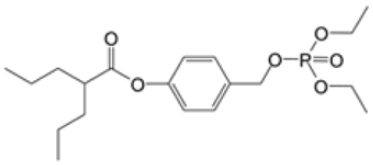

MDC-1112 (Phospho-valproic acid)

B

Cell line	24 h-IC_{50}, μM VPA	MDC-1112	Fold Enhancement
U87	1,625	64	25.4
U118	2,246	167	13.4
LN-18	2,390	137	17.4
LN-229	2,320	96	24.2

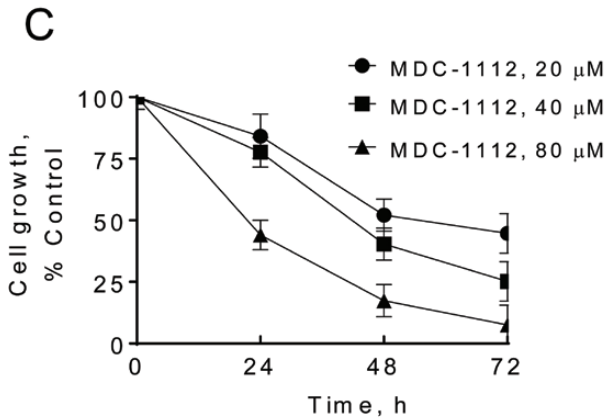

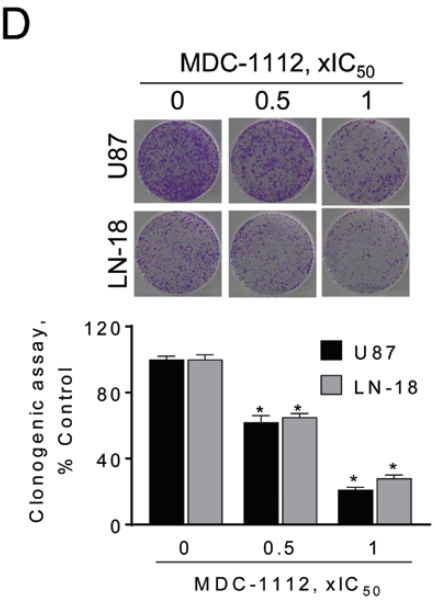

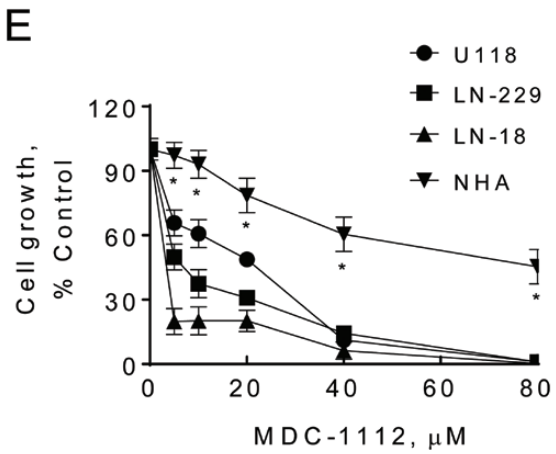

Figure 1. MDC-1112 inhibits GBM cell growth. (**A**) Chemical structure of MDC-1112 (Phospho-valproic acid). (**B**) IC_{50} values for glioblastoma cells treated with MDC-1112 or VPA for 24 h. These values are representative of three experiments, each performed in triplicates; results were within 10%. The table shows the 13.4- to 25.4-fold enhancements in potency of MDC-1112 over VPA in four human GBM cell lines. (**C**) MDC-1112 reduces human U87 cell growth in a concentration- and time-dependent manner. Results are expressed as % control. (**D**) MDC-1112 inhibits GBM cell colony formation in a concentration-dependent manner in U87 and LN-18 cells. (*$P < 0.05$, versus control). (**E**) Differential cytotoxic effect of MDC-1112 in GBM cells compared with the NHA. MDC-1112 inhibits human GBM cancer cell growth in a concentration-dependent manner. Cell growth was determined in U118, LN-229 and LN-18 GBM cells and in NHA after treatment with escalating concentrations of MDC-1112 for 48 h. Results are expressed as % control. *Significantly different compared with all other cell lines ($P < 0.05$, one-way analysis of variance test).

Western blot analysis

Following treatment with MDC-1112 at various concentrations, or for various lengths of time, cells were collected, total cell fractions obtained and western blots performed as described previously (24). Membranes were probed overnight with the following antibodies from Cell Signaling Technologies (Danvers, MA): p-$STAT3^{Ser727}$ (cat no. 9134), STAT3 (cat no. 12640), survivin (cat no. 2802), PARP (cat no. 9542), Caspase 3 (cat no. 9665), caspase 9 (cat no. 9508), p21 (cat no. 2949), p-ERK (cat no. 4370), ERK (cat no. 4675) and COX IV (cat no. 4850), or from Santa Cruz Biotechnology: HSP-60 (cat no. sc-136291) using a 1:1000 dilution of antibody in 5% (w/v) fat-free milk. β-actin (cat no. A1978 from Millipore-Sigma, Saint Louis, MO) was used as a loading control. The membranes were allowed to incubate in secondary antibody, HRP conjugated (1:5000 dilution), for 60 min. Conjugates were visualized by chemiluminescence.

Data mining analysis of STAT3

A search of genome-wide expression study with both GBM and non-tumor brain tissue yielded two independent data sets. The NCBI GEO GSE4290 data set contains 23 non-tumor samples and 81 glioblastomas. Normalized expression values from the downloaded sites were transformed to linear scale and used for statistical analysis. The TCGA GBM Affymetrix U133A data set (2013-12-18 freeze) contains 10 normal tissues and 529 primary GBM tumors. Two-tailed Welch's *t*-test

and false discovery rate calculation were performed using R and samr bioconductor package. In TCGA GBM data set, 522 GBM samples have expression data information available.

STAT3 overexpression

U118 and LN-18 cells were transiently transfected with non-specific control plasmid (control cDNA) or 100 nmol/L STAT3 expression plasmid (STAT3 cDNA; OriGene, Rockville, MD) for 48 h using Lipofectamine 3000 following the manufacturer's instructions. Following transfection, cells were replated and treated with various concentrations of MDC-1112 to determine cell growth.

Small interfering RNA gene knock-down

U118 cells were transfected with 200 ng of control or *stat3* small interfering RNA in Lipofectamine 3000 (Invitrogen), following the manufacturer's protocol. After 24 h, cells were trypsinized, and a fraction of the cells (5000 cells per well) were replated in 96-well plates and treated without or with MDC-1112 1 × IC_{50} for an additional 24 h. The remaining of the cells were used to confirm the silencing of STAT3 by western blot.

Immunohistochemistry

Immunohistochemical staining for Ki-67 and p-$STAT3^{Ser727}$ (Santa Cruz Biotechnology, Santa Cruz, CA), p21, p-$STAT3^{Tyr705}$, Bcl-xL, Mcl-1, cleaved caspase 3 and cyclin D1 (Cell Signaling Technology, Beverly MA) was performed as described previously (25).

Scoring: At least five fields per sample (at magnification ×200) were scored independently by an investigator blinded to the identity of the samples. Cells with a blue nucleus were considered unlabeled, whereas those with a brown nucleus were considered labeled. We calculated the percentage of positive cells by dividing the number of labeled cells by the number of cells in each field and multiplying by 100.

Animal studies

All animal studies were approved by our Institutional Animal Care and Use Committee.

Efficacy study in nude mouse xenografts

Female immune deficient BALB/c nude mice at 6 weeks of age were purchased from Charles River Laboratories (Wilmington, MA), and maintained in pathogen-free conditions with irradiated chow. Animals were injected bilaterally, subcutaneously with 1.5 × 10^6 U87 (study 1) or U118 (study 2) cells per side in 0.1 ml sterile phosphate-buffered saline (PBS). When the tumors became palpable, mice were divided randomly into two groups (n = 7/group), treated with vehicle control (PBS) or MDC-1112 (50 mg/kg), in PBS given i.p.1×/day, 5 days per week for 15 days (study 1) or 25 days (study 2). MDC-1112's 50 mg/kg dose represents 25% of its maximum tolerated dose, as we have determined previously (17). Body weight was determined once a week and tumor size twice weekly. Tumor size was calculated by the formula: [length × width × (length + width/2) × 0.56] in mm^3. At the end of the experiment, animals were killed by CO_2 asphyxiation and tumor weights were determined after their careful resection.

Orthotopic model of GBM and bioluminescence imaging

Female immune deficient BALB/c nude mice at 6 weeks of age were purchased from Charles River Laboratories, and maintained in pathogen-free conditions with irradiated chow. Animals were injected into the right basal ganglia of anesthetized athymic nude mice, with each mouse receiving 10 µl injections containing 0.3 ×10^6 U87-Luc cells. After a week, tumor size was monitored with bioluminensece and mice were divided randomly into two groups (n = 10–11/group), treated with vehicle control (PBS) or MDC-1112 (50 mg/kg), in PBS given i.p.1×/day, 5 days per week until killing. Body weight was determined once a week.

For bioluminescence imaging, mice were anesthetized with isoflurane, injected with 100 mg/ml D-luciferin (PerkinElmer) suspended in PBS and after 10 min intracranial tumor growth was quantified using an IVIS imaging system (PerkinElmer). Images were captured and analyzed by Living Image software (PerkinElmer).

Statistical analysis

The data, obtained from at least three independent experiments, were expressed as the mean ± SEM. Statistical evaluation was performed by one-factor analysis of variance followed by Tukey test for multiple comparisons. Kaplan–Meier analyses with log rank statistics for animal survival curves were generated using GraphPad Prism Software version 7.0.1. $P < 0.05$ was regarded statistically significant.

Results

MDC-1112 inhibits the growth of GBM cell lines more potently than VPA

To evaluate the effect of MDC-1112 on cell growth, we initially determined the 24-h IC_{50} values (drug concentration inhibiting cell growth by 50% at 24 h) of MDC-1112 and VPA in various human GBM cell lines (Figure 1B). The IC_{50} values of MDC-1112 varied among these GBM cell lines (64–167 µM), whereas those of VPA were consistently higher. In all cases, the potency of MDC-1112 was substantially greater than that of its parent compound, being enhanced between 13.4- and 25.4-fold. As shown in Figure 1C, MDC-1112 reduced U87 growth in a concentration- and time-dependent manner. Then, we examined the effect of MDC-1112 on colony formation in two GBM cell lines. MDC-1112 inhibited colony formation in a concentration-dependent manner, inhibiting colony formation in U87 and LN-18 cells by 79% and 72%, respectively ($P < 0.05$, for both), at MDC-1112 1 × IC_{50} (Figure 1D).

We next treated a panel of three human GBM cells with or without increasing concentrations of MDC-1112 (20–80 µM) for 48 h, and compared the effect of MDC-1112 on the growth of GBM cells against that of the NHA. As shown in Figure 1E, MDC-1112 reduces GBM cell growth in a concentration-dependent manner in all cell lines tested. For instance, 40 µM MDC-1112 at 48 h reduced cell growth in LN-18, LN-229 and U118 cells by 93.7%, 85.7% and 88.8% ($P < 0.05$, for all), respectively. In contrast, under the same experimental conditions, 40 µM MDC-1112 for 48 h had a lesser effect on NHA cells, reducing growth by 40.6% (Figure 1E). This indicates that MDC-1112 decreases cell growth preferentially in GBM cells compared with NHA.

MDC-1112 inhibits the growth of human GBM xenografts in nude mice

To assess the anticancer potential of MDC-1112 *in vivo*, we used heterotopic (subcutaneous) GBM xenografts in nude mice. Initially, we evaluated the chemotherapeutic effect of MDC-1112 on subcutaneous U87 xenografts. Once the tumors reached ~120 mm^3, the mice were treated intraperitoneally with either MDC-1112 50 mg/kg or vehicle. On day 15 of treatment, the tumor volume (mean ± SEM) for the vehicle control and MDC-1112 groups were 1016 ± 112 and 319.9 ± 110 mm^3, respectively, resulting in a 78% reduction in the rate of tumor growth, without signs of toxicity ($P < 0.05$; Figure 2A and B).

To rule out a cell-specific effect, we then assessed the *in vivo* chemotherapeutic potential of MDC-1112 using a human U118 GBM xenograft model. In this model, the mice were treated intraperitoneally with either MDC-1112 50 mg/kg or vehicle. At the end of the treatment (day 30), MDC-1112 inhibited U118 xenograft growth by 55% and tumor weight by 45%, compared with control ($P < 0.01$; Figure 2C and D). To note, body weight of vehicle control and MDC-1112-treated mice were comparable throughout the treatment period (Figure 2E).

To investigate the mechanism by which MDC-1112 reduced tumor growth, we determined cell proliferation (KI-67 expression), cell cycle (p21 expression) and apoptosis (cleaved caspase

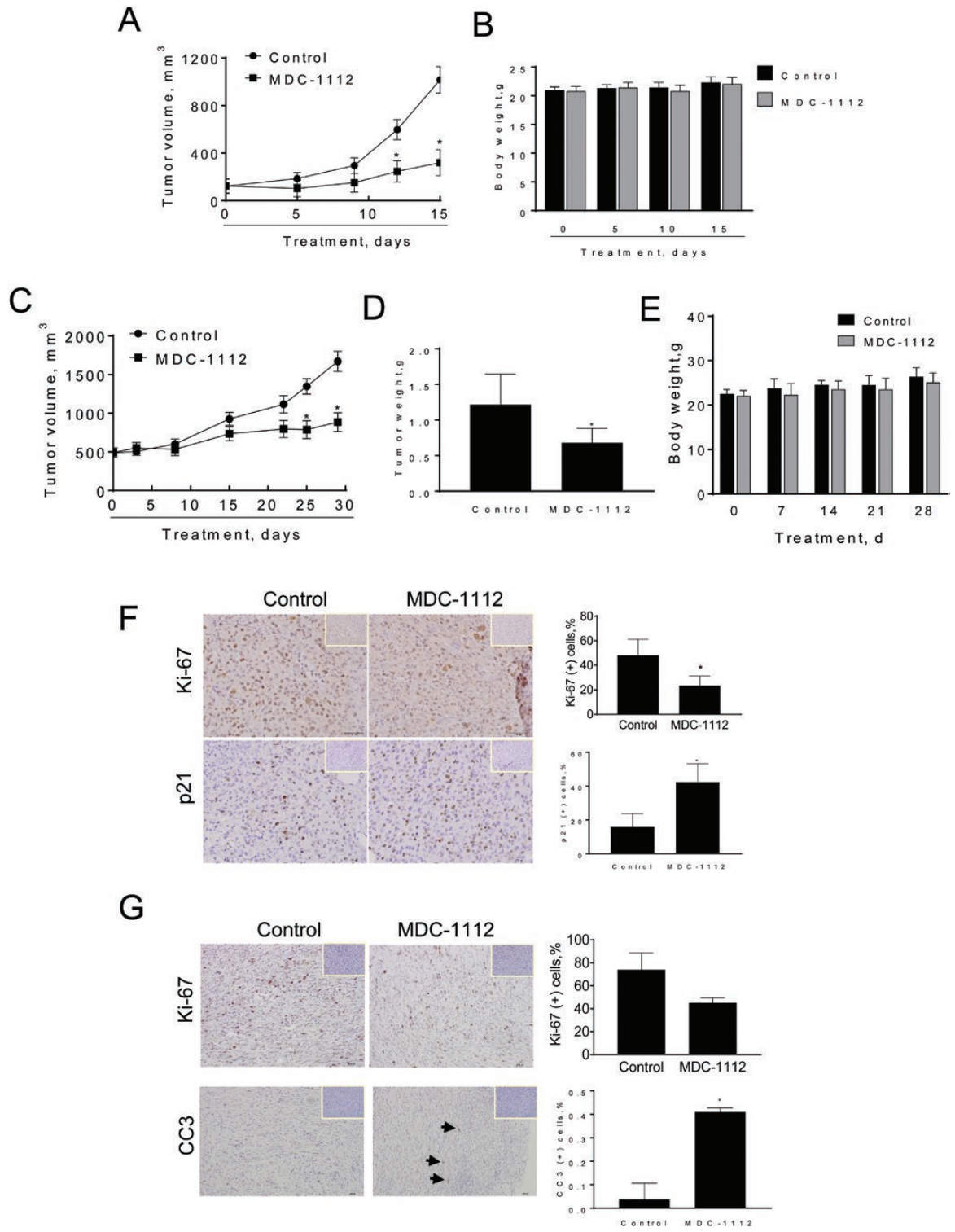

Figure 2. MDC-1112 reduces GBM xenograft growth. (**A**) MDC-1112 inhibits the growth of human U87 xenografts. U87 cells were injected s.c. into the flank areas of nude mice, and when palpable tumors were observed, the mice received MDC-1112 (50 mg/kg per day) in PBS or just PBS (control) by intraperitoneal injection for 15 days. U87 tumor volume growth over time for vehicle control- and MDC-1112-treated mice. *Significantly different compared with control group [$P < 0.01$, one-way analysis of variance (ANOVA) test]. (**B**) Mice weight progression for control and MDC-1112-treated mice. (**C**) MDC-1112 inhibits the growth of human U118 xenografts. U118 cells were injected s.c. into the flank areas of nude mice, and when palpable tumors were observed, the mice received MDC-1112 (50 mg/kg per day) in PBS or just PBS (control) by intraperitoneal injection for 30 days. U118 tumor volume growth over time for vehicle control- and MDC-1112-treated mice. *Significantly different compared with control group ($P < 0.01$, one-way ANOVA test). (**D**) Tumor weight at sacrifice. *Significantly different compared with control group ($P < 0.01$, one-way ANOVA test). (**E**) Body weight over time of mice bearing U118 xenografts treated with vehicle control (PBS) or MDC-1112 50 mg/kg. All values: mean ± SD. (**F**) Ki-67 and p21 immunostaining were performed on U87 tumor sections and photographs were taken at ×20 magnification. Representative images are shown. The consecutive section was stained with isotype IgG as negative staining control and it is shown in the upper right corner. Quantification is displayed on the right. Results were expressed as percent of Ki-67$^+$ or p21$^+$ cells ± SEM per ×20 field. *Significant compared with control group; $P < 0.05$. (**G**) Ki-67 and cleaved caspase 3 (CC3) immunostaining were performed on U118 tumor sections and photographs were taken at ×20 magnification. Representative images are shown. The consecutive section was stained with isotype IgG as negative staining control and it is shown in the upper right corner. Quantification is displayed on the right. Results were expressed as percent of Ki-67$^+$ cells ± SEM per ×20 field. *Significant compared with control group; $P < 0.05$.

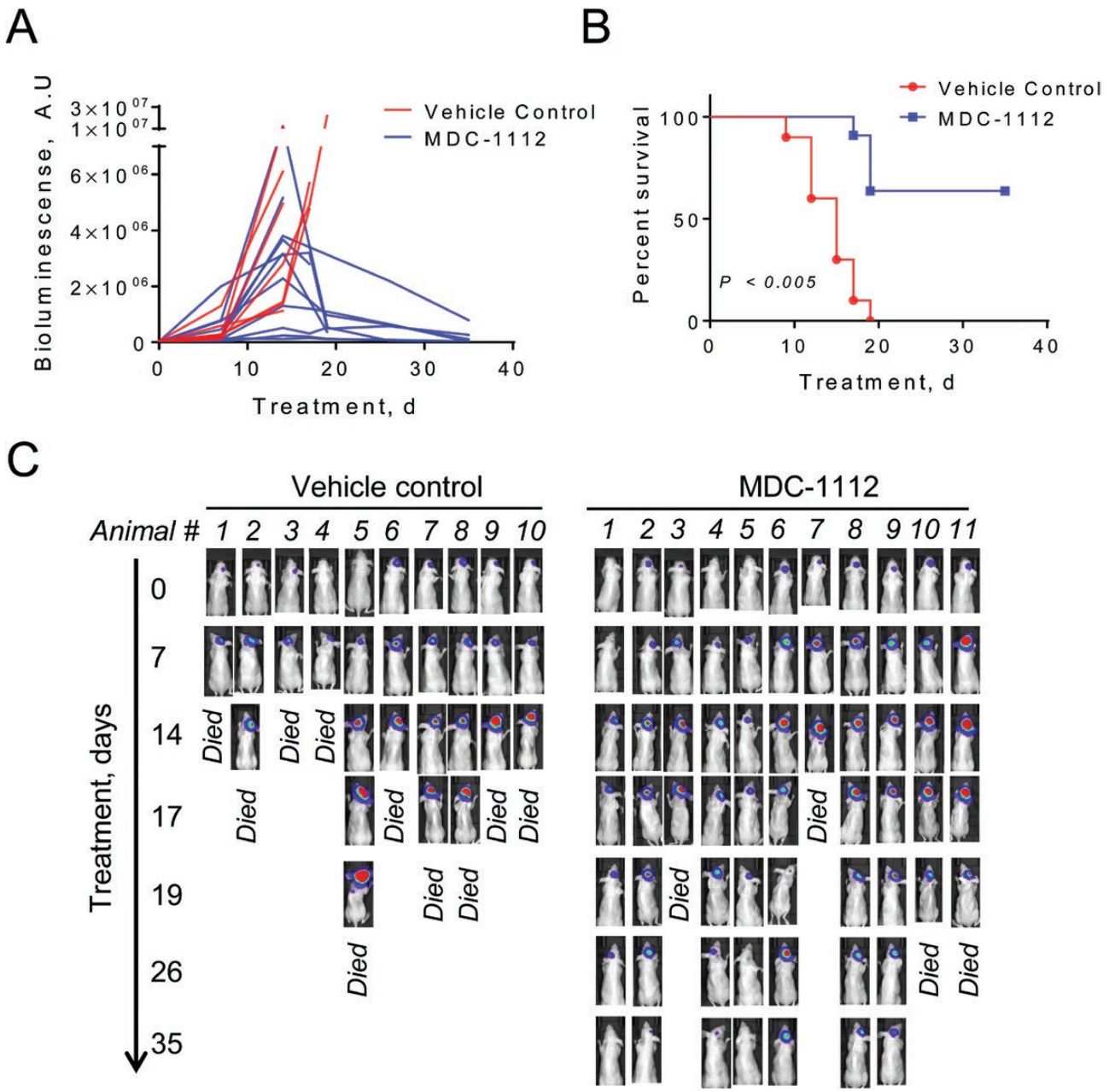

Figure 3. Treatment with MDC-1112 extends survival in mice bearing GBM intracranial tumors. (**A**) U87-Luc cells were intracranially injected, and when tumor size was confirmed by bioluminensence, mice received MDC-1112 (50 mg/kg 5×/week) in PBS or just PBS (control) by intraperitoneal injection for up to 35 days. Tumor growth over time until endpoint in vehicle control (red) or MDC-1112 (blue)-treated mice determined by bioluminescent imaging. (**B**) MDC-1112 therapy significantly prolonged survival of animals as compared with vehicle control group ($P < 0.005$). Kaplan–Meier survival curve of vehicle control (red) or MDC-1112-treated mice (blue) is shown. Seven of eleven MDC-1112-treated animals were intentionally killed (censored) for histological analysis of brain at day 35 despite being healthy. (**C**) Tumor growth was monitored by bioluminescent imaging in mice bearing intracranial U87-Luc cells (n = 10–11 per group). Representative IVIS images of U87-Luc-bearing animals over time treated as indicated.

3 expression) levels by immunohistochemistry in tumor tissue sections from control and MDC-1112-treated mice (Figure 2F and G). The expression of Ki-67 and p21 was strongly positive in the nuclei. Compared with controls, MDC-1112 inhibited cell proliferation by 52% ($P < 0.05$) and 40% in the U87 and U118 xenografts, respectively (Figure 2F and G). In addition, MDC-1112 increased the percentage of p21(+) cells by 2.6 fold and cleaved caspase 3(+) cells by 10.9-fold ($P < 0.05$; Figure 2F and G). The increase in p21 levels was also observed *in vitro*. MDC-1112 treatment led to a concentration-dependent increase in p21 expression levels in U87 cells (Supplementary Figure 1, available at *Carcinogenesis* Online).

MDC-1112 extends the survival of mice bearing intracranial tumors

We then used an intracranial orthotopic model to evaluate the anticancer effect of MDC-1112 in GBM. For this purpose, we injected U87 cells constitutively expressing luciferase (U87-Luc) in the right basal ganglia of nude mice. After 5 days, we determined the presence and size of the tumor by bioluminescence

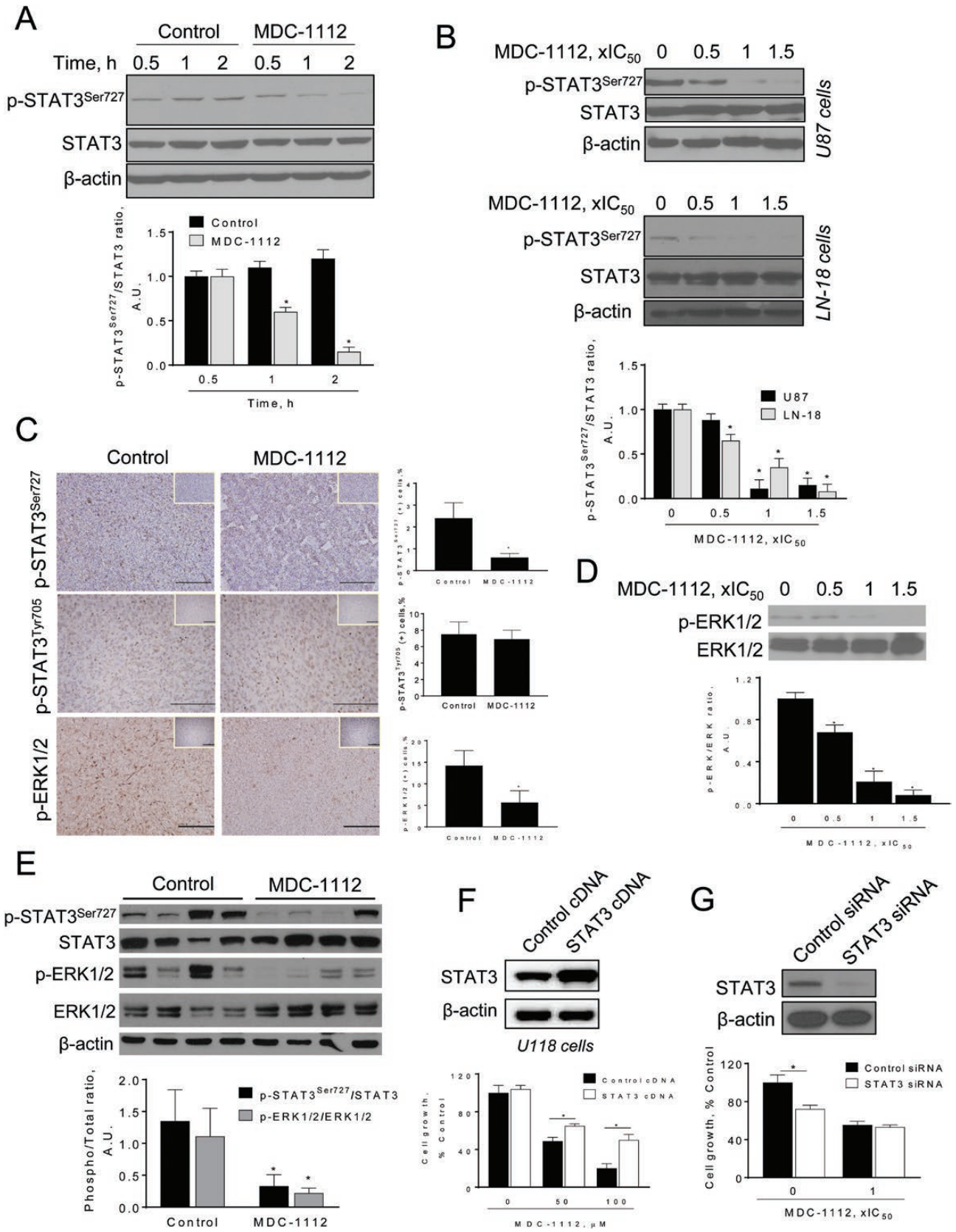

Figure 4. MDC-1112 inhibits STAT3 Ser727 signaling *in vitro* and *in vivo*. (**A**) Immunoblots of STAT3, phosphorylated STAT3 at the Ser727 residue (p-STAT3^{Ser727}), from U87 cells treated with MDC-1112, 1 × IC_{50} for different periods of time. Bands were quantified and results are shown as the ratio p-STAT3^{Ser727}:STAT3. Values are mean ± SEM. *$P < 0.05$ versus control. (**B**) Immunoblots of STAT3 and phosphorylated STAT3 at the Ser727 residue (p-STAT3^{Ser727}), from U87 and LN-18 cells treated with various concentrations of MDC-1112 for 4 h. Bands were quantified and results are shown as the ratio p-STAT3^{Ser727}:STAT3. Values are mean ± SEM. *$P < 0.05$ versus control.

and randomized the mice in vehicle-treated controls and MDC-1112-treated mice. Tumors in vehicle-treated controls grew fast (Figure 3A) and by day 19 following randomization, all mice (10 of 10) died (Figure 3B). In contrast, 7 of 11 MDC-1112-treated mice were alive at 19 days and remained alive at the end of the study (35 days of treatment; $P < 0.005$; Figure 3B and C).

MDC-1112 reduces STAT3 Ser727 signaling in GBM cells and xenografts

STAT3 plays a critical role in GBM. For example, constitutive activation of STAT3 is important in oncogenic signaling and occurs at high frequency in GBM (5,10). Furthermore, activation of STAT3 in GBM correlates with malignancy and poor prognosis.

Using publicly available data sets (NCBI GEO GSE4290 and TCGA GBM Affymetrix U133A 2013-12-18 freeze), we explored the expression status of the *stat3* gene (STAT3) in human GBM samples. STAT3 gene expression was significantly increased in GBM tumor samples compared with non-tumor samples. The fold-increase of STAT3 expression for GBM tumor/normal tissue was 2.3 (false discovery rate < 5%) and 1.5 (false discovery rate < 1%) for each data set. Moreover, GBM patients expressing higher tumor levels of STAT3 experienced worse survival than those expressing lower STAT3 tumor levels (Supplementary Figure 2A, available at *Carcinogenesis* Online), indicating that STAT3 is overexpressed in human GBM and could represent a therapeutic target.

Given that we have shown that MDC-1112 inhibits STAT3 signaling in pancreatic cancer (17), we evaluated whether MDC-1112 could inhibit STAT3 in GBM cells. We first examined the effect of MDC-1112 on STAT3 phosphorylation at the Ser727 residue, because it has been shown to influence GBM clinical outcome (14). MDC-1112 strongly inhibited STAT3 activation at the Ser727 residue, reducing its phosphorylation in a time- and concentration-dependent manner (Figure 4A and B). This was confirmed *in vivo*. Immunohistochemical studies of subcutaneous U87 xenografts revealed that MDC-1112 inhibited p-STAT3^{Ser727} expression by 75% *in vivo*, compared with control ($P < 0.05$; Figure 4C). Moreover, MDC-1112 also reduced p-STAT3^{Ser727} expression in tumor lysates (Figure 4E).

Because ERK1/2 can phosphorylate STAT3 at the Ser727 residue (26,27), we explored whether MDC-1112 affected ERK1/2 phosphorylation. In U87 cells, MDC-1112 treatment reduced p-ERK1/2 levels in a concentration-dependent manner, reducing p-ERK1/2 levels by 79% and 92% at 1 × IC_{50} and 1.5 × IC_{50}, respectively (Figure 4D). Furthermore, in U87 xenografts, MDC-1112 significantly reduced p-ERK1/2 levels by 60.5%, as shown by immunohistochemistry and immunoblotting ($P < 0.05$; Figure 4C–E).

We also examined the effect of MDC-1112 on STAT3 at the Tyr705 residue, because its phosphorylation is critical for STAT3 dimerization, nuclear translocation, and DNA binding (7). MDC-1112 failed to inhibit STAT3 phosphorylation at Tyr705 residue, nor did it reduce STAT3-dependent proteins (Figure 4C and Supplementary Figure 2B and C, available at *Carcinogenesis* Online). In GBM cells and xenografts, MDC-1112 and control groups showed similar expression levels of downstream effectors of STAT3 Tyr705, including Bcl-xL, Mcl-1, cyclin D1 and survivin (Supplementary Figure 2B and C, available at *Carcinogenesis* Online).

To evaluated whether STAT3 pathway is a key pathway of MDC-1112, we generated U118 and LN-18 cells overexpressing STAT3 (STAT3 cDNA), using as controls cells transfected with scramble cDNA (control cDNA). The overexpression of STAT3 in the GBM cells was confirmed by immunoblotting (Figure 4F). Interestingly, STAT3 overexpression abrogated, in part, the growth inhibitory effect of MDC-1112. For instance, treatment of U118 and LN-18 cells with MDC-1112 100 μM for 48 h reduced cell growth by 75% and 64%, respectively. In contrast, overexpression of STAT3 partially prevented the reduction in cell growth induced by MDC-1112 100 μM (48% and 61% of cells are viable in STAT3 overexpressing U118 and LN-18 cells at 48 h; Figure 4F and Supplementary Figure 3, available at *Carcinogenesis* Online).

To confirm the role of STAT3 in MDC-1112-induced cell growth inhibition, we silenced STAT3 in U118 cells and explored the effect of MDC-1112 on control and STAT3-silenced cells. Knocking-down *stat3* reduced U118 cell growth by 30%. In cells transfected with non-specific small interfering RNA, MDC-1112 decreased their number of viable cells by 45%, whereas in STAT3-silenced cells, MDC-1112 reduced cell growth by 47%, indicating that knocking-down *stat3* had no additional effect on the growth inhibitory effect of MDC-1112 (Figure 4G).

MDC-1112 reduces STAT3 mitochondrial levels in GBM cells

STAT3 has been shown to be present in mitochondria where it (i) regulates a metabolic function, by supporting Ras-dependent malignant transformation (8) and (ii) is important for the optimal function of the electron transport chain (9). As phosphorylation at the Ser727 residue is critical for the translocation of STAT3 into the mitochondria (27), we evaluated whether MDC-1112 affected mitochondrial STAT3 levels.

In U87 cells treated with MDC-1112 for 3 h, we observed a concentration-dependent decrease of STAT3 levels in the mitochondria (Figure 5A). This was also confirmed in U118 and LN-18 cells. On the contrary, no differences in Hsp60 chaperone protein or GRIM-19 levels were observed between the groups, indicating that the transport of these proteins was unaffected by MDC-1112.

To further evaluate the mechanism by which MDC-1112 prevents STAT3 translocation into the mitochondria, we evaluated whether MDC-1112 could affect GRIM-19, which has been shown to facilitate STAT3 entry into the mitochondria. As shown in figure 5B and C, MDC-1112 did not affect the expression GRIM-19 levels nor its mitochondrial levels.

(**C**) Immunostaining for phosphorylated STAT3 at the Ser727 residue (p-STAT3^{Ser727}) or Tyr705 residue (p-STAT3^{Tyr705}) or p-ERK1/2 expression on tissue sections of U87 tumors from control and MDC-1112-treated mice (×20). Representative images are shown. The consecutive section was stained with isotype IgG as negative staining control and it is shown in the upper right corner. Quantification is displayed on the right. Results were expressed as percent of p-STAT3^{Ser727}, p-STAT3^{Tyr705} or p-ERK1/2 positive cells per field. *Significant compared with control group; $P < 0.05$. (**D**) Immunoblots of ERK1/2 and phosphorylated ERK1/2 (p-ERK), from U87 cells treated with various concentrations of MDC-1112 for 4 h. Bands were quantified and results are shown as the ratio p-ERK:ERK. Values are mean ± SEM. *$P < 0.05$ versus control. (**E**) Immunoblots of STAT3, p-STAT3^{Ser727}, ERK1/2 and phosphorylated ERK1/2 (p-ERK), from U87 tumor lysates. Loading control: β-actin. Each lane represents a different tumor sample. Bands were quantified and results are expressed as the ratio of phospho over total expression levels for each protein. Values are mean±SEM. *$P < 0.05$ versus control. (**F**) STAT3 overexpression ameliorates, in part, the cell growth inhibition by MDC-1112. U118 cells were transfected with a control (cDNA) or STAT3-expressing plasmid for 48 h and then treated with 50 or 100 μM MDC-1112 for 48 h. Cell growth was evaluated by the MTT assay; *$P < 0.05$ versus control. Top: STAT3 expression status in whole cell protein lysates following transfection. (**G**) Effect of silencing STAT3 on MDC-1112-induced cell growth reduction. U118 cells were transfected with either control or STAT3 small interfering RNA. After transfection, cells were treated with MDC-1112 for 24 h and cell growth was evaluated; *$P < 0.05$ versus control. Immunoblots to verify STAT3 silencing were performed on whole cell extracts obtained from these cells (top panel).

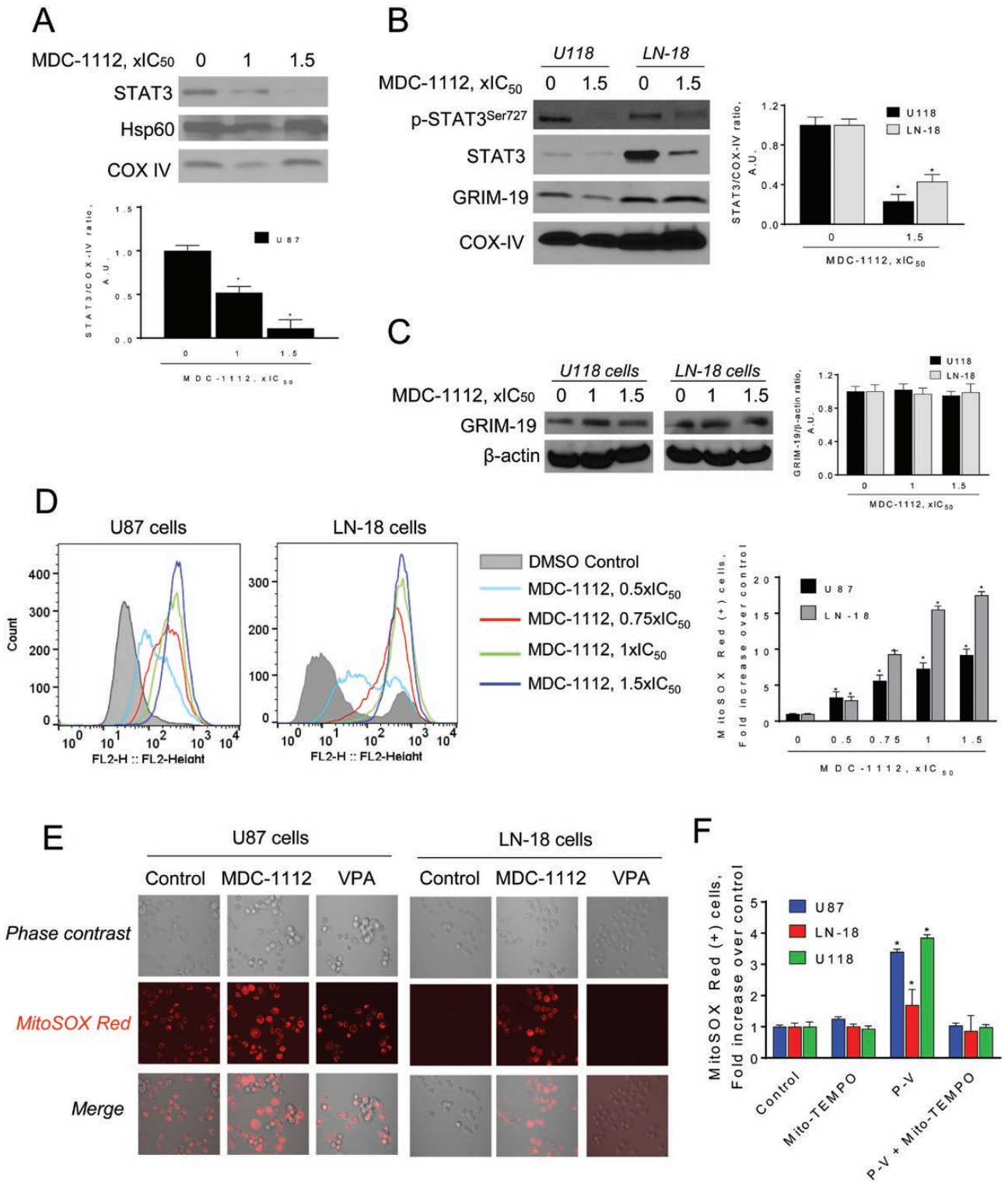

Figure 5. MDC-1112 reduces mitochondrial STAT3 levels and induces mitochondrial ROS in GBM cells. (**A**) Immunoblots for STAT3, Hsp60 or COX IV in mitochondrial (MF) fractions from U87 cells treated with MDC-1112 for 3 h. Bands were quantified and results expressed as percent control for each protein. Values are mean ± SEM. *P < 0.05 versus control. (**B**) Immunoblots for STAT3, phosphorylated STAT3 at the Ser727 residue (p-STAT3^{Ser727}), GRIM-19 and COX IV in MF from U118 and LN-18 cells treated with MDC-1112 for 3 h. Bands were quantified and results expressed as percent control for each protein. Values are mean ± SEM. *P < 0.05 versus control. (**C**) Immunoblots of GRIM-19 in total fractions from U87 cells treated with various concentrations of MDC-1112 for 4 h. Bands were quantified and results are shown as the ratio GRIM-19:β-actin. (**D**) U87 and LN-18 cells were treated with MDC-1112 for 1 h as indicated. The levels of superoxide anion in the mitochondria were determined by flow cytometry using the MitoSOX-Red fluorescent probe. Bar graph analysis of Geometric means of cells that underwent MitoSOX Red Staining. (**E**) U87 and LN-18 cells were treated without (Control) or with MDC-1112 1 × IC_{50} or VPA (1 × IC_{50}) for 1 h. Superoxide anion levels in the mitochondria was determined by confocal microscopy. Representative images are shown. (**F**) Treatment with Mito-TEMPO prevents the increase in MitoSOX-Red induced by MDC-1112 in various GBM cells. Values are mean ± SEM. *P < 0.05 versus control.

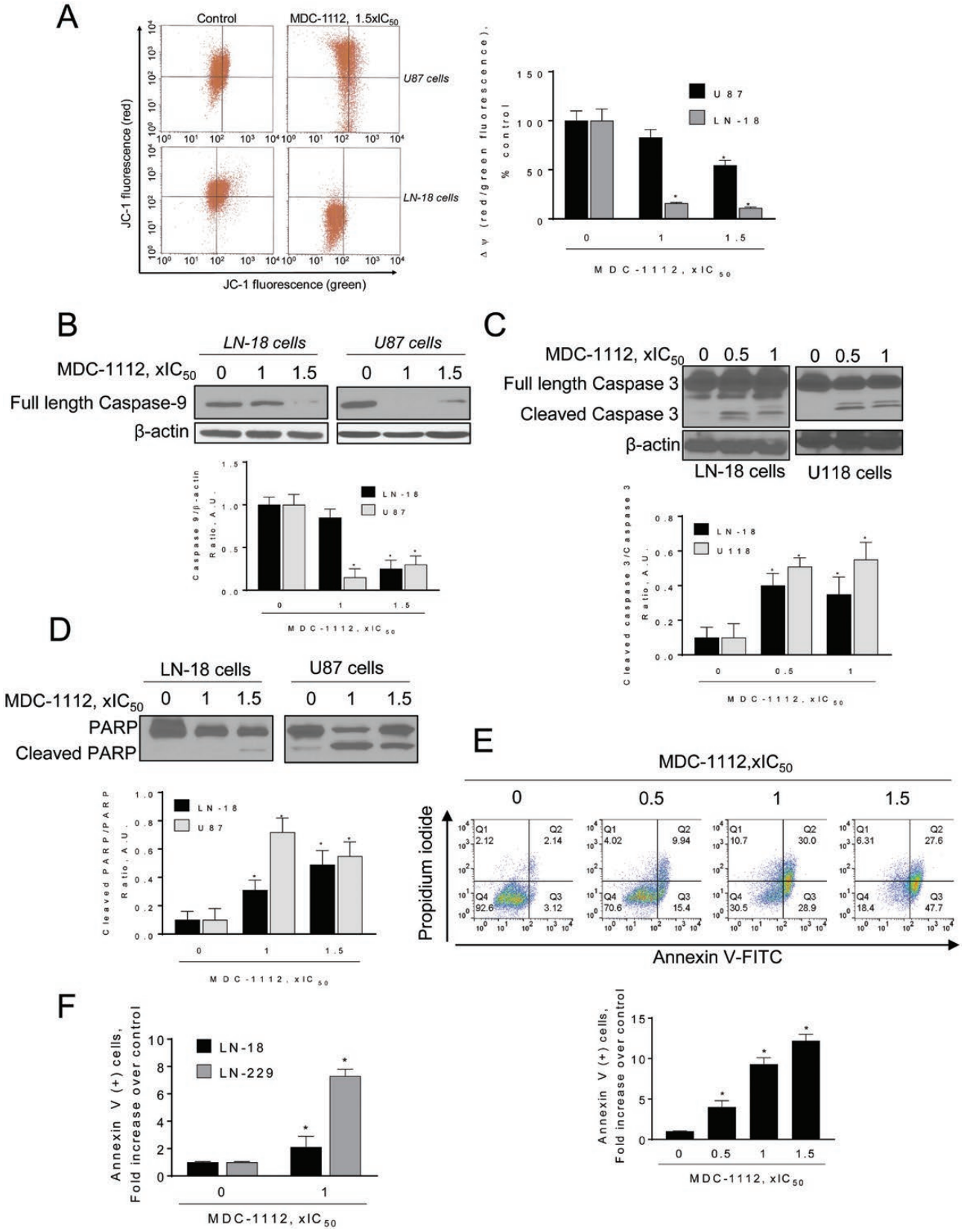

Figure 6. MDC-1112 induces intrinsic apoptosis in GBM cells. (**A**) MDC-1112 collapses the mitochondrial membrane potential (ΔΨm) in a concentration-dependent manner. Cells were stained with JC-1 and analyzed with flow cytometry after treatment with MDC-1112 for 3 h. Data were quantified and results are shown as mean ± SEM; *$P < 0.05$ versus control. (**B**) Immunoblots for full-length caspase 9 in total cell protein extracts from LN-18 or U87 cells treated with MDC-1112, as indicated, for 24 h. Loading control: β-actin. Bands were quantified and results are shown as the ratio cleaved:β-actin; *$P < 0.05$ versus control. (**C**) Immunoblots for full length and

MDC-1112 induces mitochondria ROS levels and intrinsic apoptosis in GBM cells

Given that STAT3 in the mitochondria is required for the optimal function of the electron transport chain (9), and because ROS can mediate at least part of the anticancer effect of various agents (28), we assessed whether MDC-1112 could induce the production of mitochondrial ROS in GBM cells, by determining if MDC-1112 could induce superoxide anion in mitochondria, using the selective probe MitoSOX Red. Incubation of U87 and LN-18 cells with MDC-1112 induced a concentration-dependent increase in mitochondrial superoxide anion levels (Figure 5D). This finding was confirmed by confocal microscopy (Figure 5E). In contrast to MDC-1112, VPA failed to increase mitochondrial superoxide anion (Figure 5F and Supplementary Figure 4, available at *Carcinogenesis* Online). The increase in superoxide anion levels by MDC-1112 was ameliorated by pre-treating GBM cells with the mitochondrial antioxidant TEMPO (Figure 5F).

Next, we evaluated whether MDC-1112 could affect the mitochondrial membrane potential. MDC-1112 induced a concentration-dependent decrease in mitochondrial membrane potential (Figure 6A). Incubation of U87 and LN-18 cells with MDC-1112 1 × IC_{50} and 1.5 × IC_{50} for 3 h decreased the red:green fluorescent ratio by 17% and 46% in U87 cells and by 84% and 89% in LN-18 cells, respectively, compared with controls, indicating the collapse of the mitochondrial membrane potential.

As a consequence of the aforementioned process, MDC-1112 induced the intrinsic apoptotic pathway, as shown by the cleavage of procaspase 9, following treatment with MDC-1112 (Figure 6B). This was followed by the activation of caspase 3, observed after treatment with MDC-1112 for 24 h (Figure 6C and D). To confirm the apoptotic effect of MDC-1112, we performed flow cytometry using the dual marker Annexin V/PI staining. As shown in Figure 6E, MDC-1112 strongly induced cell death by apoptosis. Treatment of U87 cells with MDC-1112 for 24 h increased the proportion of apoptotic cells in a concentration-dependent manner compared with controls. This increase became statistically significant ($P < 0.05$) at 0.5 × IC_{50} (4.0-fold over control), 1 × IC_{50} (9.3-fold over control) and 1.5 × IC_{50} (12.2-fold over control). Incubation of LN-18 and LN-229 cells with MDC-1112 1 × IC_{50} for 24 h also induced a 2.1- and 7.3-fold increase ($P < 0.05$, for both) in annexin V(+) cells, compared with controls (Figure 6F).

Discussion

Existing therapies for GBM have fallen short of improving dismal patient outcomes, with an average 15-month median overall survival. Therefore, new therapeutic strategies are critically needed to improve clinical outcome. Our results establish MDC-1112 as a strong inhibitor of GBM growth in preclinical models, whose distinct mechanism of action is dominated by inhibition of STAT3 at the Ser727 residue. All these attributes make MDC-1112 a promising candidate drug for the treatment of GBM.

A common practice in drug development involves exploiting the properties of putative molecular targets. We have modified VPA to generate MDC-1112 (phospho-valproic acid) in such a way as to enhance its pharmacological properties, in particular its efficacy (17). The present results establish MDC-1112 as an agent with significantly improved anticancer activity over its parent compound VPA. MDC-1112 is a potent inhibitor of GBM cell growth *in vitro* (>13.4-fold more potent than VPA). *In vivo*, MDC-1112 suppressed the growth of subcutaneous U87 and U118 tumors in immunodeficient mice, and this effect was characterized by decreased cell proliferation and increased apoptosis. Furthermore, MDC-1112 extended the survival of mice bearing intracranial GBM tumors, with some tumors regressing in size. Importantly, MDC-1112 was safe, showing essentially no signs of toxicity in GBM mouse models. This finding is in agreement with our previous report showing that MDC-1112 lacked genotoxicity and was well tolerated (17), highlighting MDC-1112's safety in multiple animal models of disease. These results indicate that MDC-1112 is a promising agent for GBM treatment.

An important feature of an anticancer drug is its selectivity. Anticancer drugs should preferentially target the tumor and not the normal surrounding tissue. MDC-1112 displays such selectivity. Compared with several GBM cell lines, normal human astrocytes, e.g. NHA cells, were more resistant to MDC-1112-suppression of their growth. Such selectivity, if broadly confirmed, will be a significant advantage of MDC-1112.

STAT3 is an important oncogenic signaling molecule, found to be activated at high frequency in human cancers, including GBM (5,10). Because the activation of STAT3 in GBM correlates with malignancy and poor prognosis (11–13), there have been multiple efforts, including ours, to develop and evaluate anticancer drugs that target STAT3 during the last years (29–31). The molecular mechanism underlying the anticancer effect of MDC-1112 is dominated by its ability to inhibit STAT3, which is supported by two findings: (i) that STAT3 overexpression ameliorated the anticancer effect of MDC-1112 and (ii) the fact that silencing STAT3 did not lead to additional growth inhibitory effect by MDC-1112.

However, to our surprise, the main STAT3 target was not the inhibition of STAT3 activation at the Tyr705 residue, a residue important for nuclear translocation of STAT3 and its function as a transcription factor, and which we have shown to be affected by MDC-1112 in pancreatic cancer (17). At present, there is no readily explanation for this seemingly discrepancy regarding the effect of MDC-1112 on the phosphorylation of STAT3 Tyr705 residue in pancreatic cancer and GBM. On the contrary, MDC-1112 strongly inhibited STAT3 phosphorylation at the Ser727 residue, which appears to be the key residue affected by MDC-1112 in GBM and in pancreatic cancer. As Ser727 phosphorylation is achieved by serine/threonine kinases, including ERK1/2 (27), the inhibition of STAT3 Ser727 phosphorylation is due in part by the inhibition of ERK phosphorylation by MDC-1112, as shown *in vitro* and *in vivo*.

High expression levels of phosphorylated STAT3, at both Tyr705 and Ser727 residues, are predictive of poorer clinical outcome in GBM patients. However, only the high proportion of phosphorylated STAT3 Ser727 positive neoplastic cells in GBM were shown to be an independent unfavorable prognostic factor (14). Therefore, MDC-1112 by targeting STAT3 at the

cleaved caspase 3 in total cell protein extracts from LN-18 or U118 cells treated with MDC-1112, as indicated, for 24 h. Loading control: β-actin. Bands were quantified and results are shown as the ratio cleaved:full length protein; *$P < 0.05$ versus control. (**D**) Immunoblots for full length and cleaved PARP in total cell protein extracts from LN-18 or U87 cells treated with MDC-1112, as indicated, for 24 h. Bands were quantified and results are shown as the ratio cleaved/full length protein; *$P < 0.05$ versus control. (**E**) Cell death by apoptosis was determined by flow cytometry using the dual staining (Annexin V and PI) in U87 cells treated with increasing concentrations of MDC-1112 for 24 h. Results are expressed as fold-increase compared with the percentage of Annexin V (+) cells in the control group. (**F**) Cell death by apoptosis was determined by flow cytometry in LN-18 and LN-229 cells incubated without or with MDC-1112 1 × IC_{50} for 24 h. Results are expressed as fold-increase compared with the percentage of apoptotic cells in the control group.

critical Ser727 residue may offer a useful avenue for therapeutic intervention.

The phosphorylation state of STAT3 at the Ser727 residue mediates the actions of mitochondrial STAT3 (32). The reduction of mitochondrial STAT3 by MDC-1112 had serious implications because STAT3 regulates cellular respiration in mitochondria (9). The decrease in STAT3 levels was responsible for the enhanced generation of O_2^- selectively by the mitochondria, and the resultant oxidative stress triggered the intrinsic apoptotic cascade of the GBM cells, manifested by the collapse of the mitochondrial membrane potential and the downstream activation of execution caspases. STAT3 disruption was reported to decrease mitochondrial function and increase oxidative stress in astrocytes (33) and cardiomyocytes (34,35). In agreement with our findings, Zhang *et al.*(32) have shown that mitochondrial STAT3 is critical in promoting breast cancer growth, and the functional presence of STAT3 in mitochondria reduces ROS and allows the proper functioning of the electron transport chain. These results indicate that targeting STAT3 at the mitochondrial level may represent a potential therapeutic strategy.

In conclusion, MDC-1112 is an effective anticancer agent in preclinical models of GBM, is selective towards GBM cells versus NHA, and STAT3 at the Ser727 residue represents a key molecular target for its effect. Therefore, MDC-1112 deserves further investigation as a potential agent for GBM treatment.

Supplementary material

Supplementary data are available at *Carcinogenesis* online.

Funding

Stony Brook Cancer Center; the University of California, Davis; NIH CA (R21 175699, R03 181727 to G.G.M.); the National Institutes of Health Bridges to the Baccalaureate program (R25-GM050070 to J.M. and L.M.).

Conflict of Interest Statement: B.R. has an equity position in Medicon Pharmaceuticals, the company that owns the test compound. All other authors declare no competing financial interest.

References

1. Tykocki, T. *et al.* (2018) Ten-year survival in glioblastoma. A systematic review. *J. Clin. Neurosci.*, 54, 7–13.
2. Nagasawa, D.T. *et al.* (2012) Temozolomide and other potential agents for the treatment of glioblastoma multiforme. *Neurosurg. Clin. N. Am.*, 23, 307–22, ix.
3. Stupp, R. *et al.*; European Organisation for Research and Treatment of Cancer Brain Tumor and Radiotherapy Groups; National Cancer Institute of Canada Clinical Trials Group. (2005) Radiotherapy plus concomitant and adjuvant temozolomide for glioblastoma. *N. Engl. J. Med.*, 352, 987–996.
4. Patel, M.A. *et al.* (2014) The future of glioblastoma therapy: synergism of standard of care and immunotherapy. *Cancers (Basel).*, 6, 1953–1985.
5. Kim, B.H. *et al.* (2016) Signal transducer and activator of transcription 3 as a therapeutic target for cancer and the tumor microenvironment. *Arch. Pharm. Res.*, 39, 1085–1099.
6. Benekli, M. *et al.* (2003) Signal transducer and activator of transcription proteins in leukemias. *Blood*, 101, 2940–2954.
7. Holtick, U. *et al.* (2005) STAT3 is essential for Hodgkin lymphoma cell proliferation and is a target of tyrphostin AG17 which confers sensitization for apoptosis. *Leukemia*, 19, 936–944.
8. Gough, D.J. *et al.* (2009) Mitochondrial STAT3 supports Ras-dependent oncogenic transformation. *Science*, 324, 1713–1716.
9. Wegrzyn, J. *et al.* (2009) Function of mitochondrial Stat3 in cellular respiration. *Science*, 323, 793–797.
10. Gray, G.K. *et al.* (2014) NF-κB and STAT3 in glioblastoma: therapeutic targets coming of age. *Expert Rev. Neurother.*, 14, 1293–1306.
11. Gong, A.H. *et al.* (2015) FoxM1 drives a feed-forward STAT3-activation signaling loop that promotes the self-renewal and tumorigenicity of glioblastoma stem-like cells. *Cancer Res.*, 75, 2337–2348.
12. Lo, H.W. *et al.* (2008) Constitutively activated STAT3 frequently coexpresses with epidermal growth factor receptor in high-grade gliomas and targeting STAT3 sensitizes them to Iressa and alkylators. *Clin. Cancer Res.*, 14, 6042–6054.
13. Abou-Ghazal, M. *et al.* (2008) The incidence, correlation with tumor-infiltrating inflammation, and prognosis of phosphorylated STAT3 expression in human gliomas. *Clin. Cancer Res.*, 14, 8228–8235.
14. Lin, G.S. *et al.* (2014) STAT3 serine 727 phosphorylation influences clinical outcome in glioblastoma. *Int. J. Clin. Exp. Pathol.*, 7, 3141–3149.
15. Han, T.J. *et al.* (2016) Inhibition of STAT3 enhances the radiosensitizing effect of temozolomide in glioblastoma cells *in vitro* and *in vivo*. *J. Neurooncol.*, 130, 89–98.
16. Kim, J.E. *et al.* (2014) STAT3 Activation in Glioblastoma: Biochemical and Therapeutic Implications. *Cancers (Basel).*, 6, 376–395.
17. Mackenzie, G.G. *et al.* (2013) Targeting mitochondrial STAT3 with the novel phospho-valproic acid (MDC-1112) inhibits pancreatic cancer growth in mice. *PLoS One*, 8, e61532.
18. Huang, L. *et al.* (2011) Chemotherapeutic properties of phospho-nonsteroidal anti-inflammatory drugs, a new class of anticancer compounds. *Cancer Res.*, 71, 7617–7627.
19. Mackenzie, G.G. *et al.* (2010) Phospho-sulindac (OXT-328), a novel sulindac derivative, is safe and effective in colon cancer prevention in mice. *Gastroenterology*, 139, 1320–1332.
20. Mackenzie, G.G. *et al.* (2013) A novel Ras inhibitor (MDC-1016) reduces human pancreatic tumor growth in mice. *Neoplasia*, 15, 1184–1195.
21. Franken, N.A. *et al.* (2006) Clonogenic assay of cells *in vitro*. *Nat. Protoc.*, 1, 2315–2319.
22. Sun, Y. *et al.* (2008) The thioredoxin system mediates redox-induced cell death in human colon cancer cells: implications for the mechanism of action of anticancer agents. *Cancer Res.*, 68, 8269–8277.
23. Zhao, W. *et al.* (2009) Phosphoaspirin (MDC-43), a novel benzyl ester of aspirin, inhibits the growth of human cancer cell lines more potently than aspirin: a redox-dependent effect. *Carcinogenesis*, 30, 512–519.
24. Mackenzie, G.G. *et al.* (2008) Curcumin induces cell-arrest and apoptosis in association with the inhibition of constitutively active NF-kappaB and STAT3 pathways in Hodgkin's lymphoma cells. *Int. J. Cancer*, 123, 56–65.
25. Mackenzie, G.G. *et al.* (2011) Phospho-sulindac (OXT-328) combined with difluoromethylornithine prevents colon cancer in mice. *Cancer Prev. Res. (Phila).*, 4, 1052–1060.
26. Yang, R. *et al.* (2016) Mitochondrial Stat3, the need for design thinking. *Int. J. Biol. Sci.*, 12, 532–544.
27. Gough, D.J. *et al.* (2013) The MEK-ERK pathway is necessary for serine phosphorylation of mitochondrial STAT3 and Ras-mediated transformation. *PLoS One*, 8, e83395.
28. Rigas, B. *et al.* (2008) Induction of oxidative stress as a mechanism of action of chemopreventive agents against cancer. *Br. J. Cancer*, 98, 1157–1160.
29. de Groot, J. *et al.* (2012) Modulating antiangiogenic resistance by inhibiting the signal transducer and activator of transcription 3 pathway in glioblastoma. *Oncotarget*, 3, 1036–1048.
30. Heimberger, A.B. (2011) The therapeutic potential of inhibitors of the signal transducer and activator of transcription 3 for central nervous system malignancies. *Surg. Neurol. Int.*, 2, 163.
31. Lin, L. *et al.* (2010) A novel small molecule, LLL12, inhibits STAT3 phosphorylation and activities and exhibits potent growth-suppressive activity in human cancer cells. *Neoplasia*, 12, 39–50.
32. Zhang, Q. *et al.* (2013) Mitochondrial localized Stat3 promotes breast cancer growth via phosphorylation of serine 727. *J. Biol. Chem.*, 288, 31280–31288.
33. Sarafian, T.A. *et al.* (2010) Disruption of astrocyte STAT3 signaling decreases mitochondrial function and increases oxidative stress *in vitro*. *PLoS One*, 5, e9532.
34. Szczepanek, K. *et al.* (2011) Mitochondrial-targeted Signal transducer and activator of transcription 3 (STAT3) protects against ischemia-induced changes in the electron transport chain and the generation of reactive oxygen species. *J. Biol. Chem.*, 286, 29610–29620.
35. Szczepanek, K. *et al.* (2012) Cytoprotection by the modulation of mitochondrial electron transport chain: the emerging role of mitochondrial STAT3. *Mitochondrion*, 12, 180–189.